Full length article

Generalized Gibbs-Thomson equation for nanoparticles at grain boundaries

M. Lin [a, c], G. Gottstein [a, *, 1], L.S. Shvindlerman [a, b]

[a] Institut für Metallkunde und Metallphysik, RWTH Aachen University, Kopernikusstr. 14, Aachen, Germany
[b] Institute of Solid State Physics, Russian Academy of Sciences, Chernogolovka, Moscow Distr., Russia
[c] Institut für Eisenhüttenkunde, RWTH Aachen University, Intzestr. 1, Aachen, Germany

ABSTRACT

A general Gibbs-Thomson equation is derived from the complete free energy description of precipitates at grain boundaries, taking into account the excess free energy of the grain boundary − phase boundary junction. In this model, the equilibrium shape of particles shows a strong dependency on the particle size, which gives rise to a deviation from the classical theory of precipitation. The influence of the line tension of triple junctions on the nucleation energy barrier is discussed.

© 2017 Acta Materialia Inc. Published by Elsevier Ltd. All rights reserved.

1. Introduction

Precipitation is a common form of phase transformation in nature: from water droplets in clouds to second-phase particles in metals. The new phase is dispersed in the form of small particles in the mother phase and its total volume fraction is so small that the coalescence of different particles can be neglected. In a classical model of precipitation, a second-phase particle is treated as a sphere separated from the matrix by a phase boundary, whose excess energy gives rise to a nucleation barrier. In heterogeneous systems, nuclei are formed preferentially at certain locations with a low energy barrier. An important kind of nucleation site in a polycrystalline material is a grain boundary. It is commonly observed that the grain interior in the vicinity of a grain boundary is free of precipitates. One can expect that the precipitate-free-zone (PFZ) can cover the whole grain interior when the grain size falls below a certain value. In this case the precipitation at grain boundaries becomes dominant.

Second-phase particles formed at grain boundaries are accompanied by a special line defect, the triple junction (TJ) where the phase boundary and the grain boundary meet. At the junction the atoms should rearrange to accommodate the lattice- and orientation differences of the three adjoining crystals and, consequently, may increase or decrease the total free energy. The line tension of a TJ, which is defined as the excess free energy with respect to the length of the TJ line, was first introduced by Gibbs [1] and recently accurately measured [2,3]. Also, molecular dynamics (MD) simulations were carried out to estimate the excess energy of a three-grain-boundary junction [4−7].

An analogon to a TJ in a liquid system is a three phase contact line (TPCL) at the bottom of a droplet on a solid substrate. The dependency of the contact angle at the TPCL on its curvature has been studied extensively in sessile droplet experiments. The Young equation, which describes the relation between contact angle θ and surface energy γ, was modified to take this phenomenon into account. A new parameter, the "line tension" τ, whose concept was first introduced by Gibbs [1], has been introduced to represent a curvature-dependent "force" on the TPCL. The modified Young equation for a droplet on a flat horizontal substrate [8−10] reads

$$\cos \theta = \frac{\gamma_{sg} - \gamma_{sl} - \tau/r}{\gamma_{lg}} \tag{1}$$

where γ_{ij} are the surface tensions of the solid-gas (sg), solid-liquid

* Corresponding author.
  E-mail address: gottstein@imm.rwth-aachen.de (G. Gottstein).
[1] This author was an Editor of the journal during the review period of the article. To avoid a conflict of interest, Christopher A. Schuh acted as Editor for this manuscript.

(sl) and liquid-gas (lg) interfaces, respectively; r is the radius of curvature of the TPCL, and τ is the line tension.

Both positive and negative values of TPCL tension were reported. In some sessile droplet experiments [11,12], smaller droplets showed stronger wetting (smaller contact angle) than predicted by the Young equation, which implies a negative line tension. In the MD simulations of symmetric-tilt-grain-boundary junctions by Srinivasan et al. [5] and Eich et al. [4], the TJ excess energy was found to be potentially negative.

Both the magnitude and the sign of the line tension are under controversy [13–15]. Deviation from the modified Young equation for submicrometer sessile droplets has been shown by accurate measurements on the contact angle [11,12,14]. Nevertheless, it is certain that the contact angle can change in both directions with the triple-junction curvature whose dependency can be semi-quantitatively described by the modified Young equation. Complete wetting or dewetting can be expected when the size of a droplet or particle approaches zero.

The quantity corresponding to τ in a solid material is the "triple-junction energy". In this text, we use the terms "line tension" and "triple junction energy" interchangeably. The experimental results on pure copper and copper alloys yielded a positive triple junction energy. However, there is no proof that the triple junction energy in other solids cannot be negative. This excess energy is an extra driving force for microstructural restoration processes, such as grain growth or precipitation, which has not been considered in conventional theories.

A triple line cannot exist independently of grain- or phase boundaries. It is therefore natural to express the triple line tension in relation to the excess interfacial free energy. A dimensional analysis yields that the ratio of the line tension τ to the surface energy γ_s has the dimension of a length. We introduce the quantity

$$r^* = \frac{\tau}{\gamma_s} \tag{2}$$

as a measure for the line tension of triple junctions and refer to it as "characteristic length". By applying this quantity to the modified Young equation, the curvature-dependent term $\tau/\gamma r$ can be simplified to r^*/r, which will vanish for $r \gg r^*$. Thus, the characteristic length r^* is the length scale on which the triple junction energy is not negligible. Zhao et al. [2,3] measured the curvature dependency of the dihedral angle at thermal grooves using atomic force microscopy and determined the line tension of the GB-surface triple junction, i.e. the groove root to be $(2.5\pm1.1) \times 10^{-8} J/m$. According to this measurement the characteristic length of the TJ tension is of the order of nanometers. In the following we shall investigate the effect of triple-junctions on precipitation at grain boundaries.
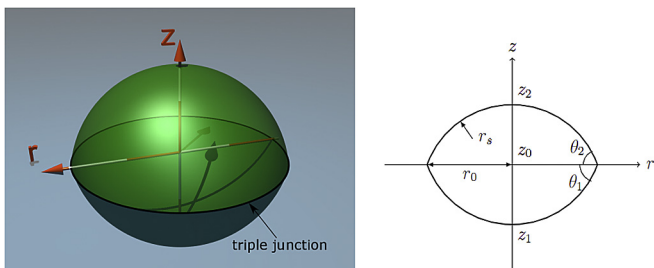
2. Equilibrium shape of a particle at a grain boundary

Let us consider a second phase particle located at a grain boundary as shown in Fig. 1. Part of the grain boundary is replaced by the particle and a circular triple line is formed. Assuming that the grain boundary and TJ properties are isotropic, the particle should have rotation symmetry. Taking into account the contribution of the TJ excess energy τ, we can formulate the total free energy of the particle as

$$G = 2\pi \int_{x_1}^{x_2} \left(\gamma_s r \sqrt{1 + r'^2} - \Delta p \frac{r^2}{2} \right) dx + 2\pi \tau r_0 - \gamma_b \pi r_0^2 \tag{3}$$

where γ_s and γ_b are the phase boundary energy and grain boundary energy, respectively. Δp represents the general volumetric (bulk) driving force. If we only consider the chemical contribution, $\Delta p = (g_{\text{matrix}} - g_{\text{precipitate}})/V_{\text{precipitate}}^m$, where g denotes the effective molar free energy and V^m is the molar volume. For the precipitation of vacancies, the numerator in the expression should be replaced by the chemical potential of vacancies μ_v, that is $\Delta p = \mu_v / V_v^m$.

We derive the Euler equation and the transversality equations from the first-order variation of G.

$$\frac{1}{2\pi} \delta G = \int_{x_1}^{x_2} \left(F_r - \frac{d}{dx} F_{r'} \right) \delta r dx + \left[F_{r'} |_{x_0+0}^{x_0-0} + (\tau - \gamma_b r_0) \right] dr_0$$
$$+ (F - r' F_{r'})|_{x_0+0}^{x_0-0} dx_0 \tag{4}$$

where $F(r, r') = \gamma_s r \sqrt{1 + r'^2} - \frac{\Delta p}{2} r^2$. The variation δG must be zero for an arbitrary variation δr, dr_0 and dx_0, hence

$$\frac{\Delta p}{\gamma_s} = \frac{r''}{\left(1 + r'^2\right)^{3/2}} + \frac{1}{r\sqrt{1 + r'^2}} \tag{5}$$

$$0 = \gamma_s \frac{r'}{\sqrt{1 + r'^2}} \bigg|_{x_0+0}^{x_0-0} + \frac{\tau}{r_0} - \gamma_b \tag{6}$$

$$0 = \frac{\gamma_s}{\sqrt{1 + r'^2}} \bigg|_{x_0+0}^{x_0-0} \tag{7}$$

The first equation is the Euler equation. The second and third equation are the transversality conditions. Note that the right hand side of Eq. (5) is equal to two times of the mean curvature of the surface obtained by rotating the curve $r(x)$. Supposed that surface energy and driving force are constant for the upper and lower cap, these two caps should be Constant-Mean-Curvature (CMC) surfaces. The CMC surfaces with circular symmetry are known as Delaunay surfaces in geometry [16], such as plane, sphere, cylinder and catenoid.

Integrating $r(x)$ with the initial condition $r(x_1) = 0$ and $r'(x_1) = \infty$ yields a circle.

$$r = \sqrt{r_s^2 - (r_s + x_1 - x)^2} \tag{8}$$

The radius r_s is defined as the radius of curvature of the particle surface. We can derive from Eq. (5) that $r_s = \frac{2\gamma_s}{\Delta p}$.

Substituting the derivatives r' by trigonometric functions of the contact angles, the equations of the transversality conditions can be transformed to

Fig. 1. Shape of a precipitate situated on grain boundary; the blue plane represents the grain boundary and the green surfaces represent the phase boundary.

$$\gamma_1 \cos \theta_1 + \gamma_2 \cos \theta_2 + \tau/r_0 - \gamma_b = 0 \tag{9a}$$

$$\gamma_1 \sin \theta_1 - \gamma_2 \sin \theta_2 = 0 \tag{9b}$$

In the current study, we just consider the simplest case that the surface energies of the upper and lower cap are equal, $\gamma_1 = \gamma_2 = \gamma_s$, so the two equations can be reduced to a single expression

$$\cos \theta = \frac{\gamma_b - \tau/r_0}{2\gamma_s} \tag{10}$$

where $\theta = \theta_1 = \theta_2$. With the geometric relationship $r_0 = r_s \sin \theta$, the radius of curvature r_s of the particle surface can be expressed as

$$r_s = r_0 \left[1 - \left(\frac{\gamma_b - \tau/r_0}{2\gamma_s} \right)^2 \right]^{-\frac{1}{2}} \tag{11}$$

Fig. 2 shows the equilibrium shapes of particles of different sizes relative to the characteristic length $r^* = \frac{\tau}{\gamma_s}$.

Summarizing the Euler- and the transversality equations, the minimum value for the functional $G[r(z)]$ reads

$$G_{\min} = \left(\frac{2\tau}{r_0} - \gamma_b + \frac{4\gamma_s}{1 + \cos \theta} \right) \pi r_0^2 - \Delta p V \tag{12}$$

where

$$V = \frac{2\pi}{3} r_0^3 \frac{(1 - \cos \theta)(2 + \cos \theta)}{\sin \theta (1 + \cos \theta)} \tag{13}$$

According to the Gibbs-Thomson equation, the concentration of solute atoms near the surface of a particle of finite volume is

$$c_i = c_\infty \exp \left(\frac{\Delta p_e \Omega}{kT} \right) \tag{14}$$

where c_∞ stands for the equilibrium concentration near an infinitely large particle; Ω is the effective atomic volume; and Δp_e is the bulk driving force that satisfies the equilibrium condition, $G'_{\min}(V) = 0$. Analogous to the classical derivation of the Gibbs-Thomson equation, Δp_e corresponds to the shift of bulk free energy of the precipitate (Fig. 3). It reduces to $2\gamma_s/r$ for a spherical particle in the bulk and yields the classical Gibbs-Thomson relation.

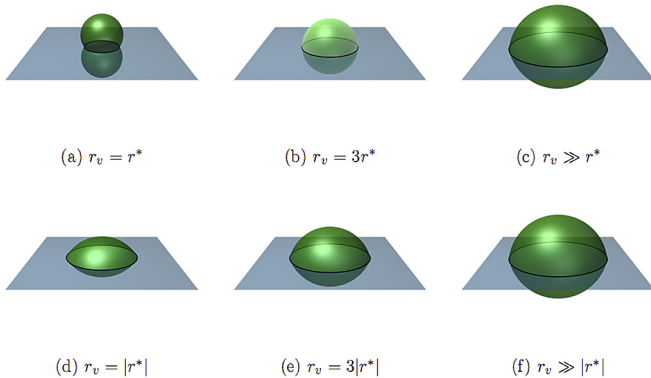By combining Eqs. (8), (10) and (14) we obtain

Fig. 2. Equilibrium shapes of particles with different volume and triple junction tension. (a–c): positive TJ tension, $r^* > 0$; (d–e): negative TJ tension, $r^* < 0$. r_v is the equivalent spherical radius. $\gamma_s/\gamma_b = 3$.
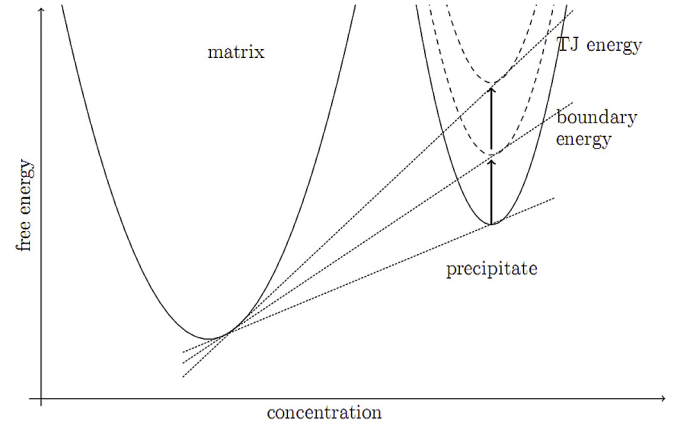

Fig. 3. Schematic Gibbs free energy diagram illustrating the effect of boundary energy and triple-junction energy on the concentration at the precipitate surface.

$$c_i = c_\infty \exp \left(\frac{2\gamma_s \Omega}{kTr_s} \right) = c_\infty \exp \left(\frac{2\gamma_s \Omega}{kTr_0} \cdot \sqrt{1 - \left(\frac{\gamma_b - \tau/r_0}{2\gamma_s} \right)^2} \right) \tag{15}$$

The dependency $c_i(V)$ cannot be expressed analytically. Its numerical solutions are shown in Fig. 4. If the contact angle is assumed to be constant, the classical Gibbs-Thomson relation ($r^* = 0$) is represented by $c_i \sim 1/r_v$. When the particle size is comparable to r^*, the constancy of the contact angle breaks down due to the TJ tension. Therefore, the modified Gibbs-Thomson relation $c_i(r_v)$ deviates from the classical relation. Fig. 4 shows that a positive TJ energy ($r^* > 0$) increases the concentration slightly and a negative TJ energy ($r^* < 0$) decreases it significantly.

The Gibbs-Thomson equation is fundamental to many existing models for the nucleation, growth and coarsening of second phase particles (or voids). According to the measurement of Zhao et al. [2,3] in pure Cu, the line tension of the TJ between GB and free surface is 25±11 J/nm. Thus, the characteristic length r^* for voids in polycrystalline Cu is between 10 and 30 nm. This result gives reason to reconsider the Gibbs-Thomson effect for voids smaller than 10 nm.

Anisotropy plays an important role in most real scenarios of GB precipitation. An interesting direction of extension to the current model is to include the inclination dependency of the phase
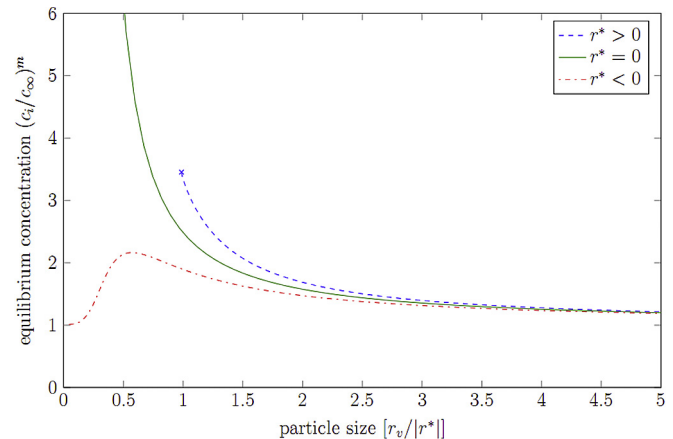

Fig. 4. Gibbs-Thomson relation for particles of size r_v with different triple junction tension; $r_v \equiv \sqrt[3]{3V/4\pi}$; $m \equiv \frac{kTr^*}{2\gamma_s\Omega}$; $r \equiv \tau/\gamma_s$ s; $\gamma_b = \gamma_s/3$.

boundary energy and the TJ energy, which will result in facets on the surface of the particles. The problem will not be solvable by analytical methods and requires a complete 3 dimensional description of the interfaces and TJs. Various numerical methods can be employed: Both the multi-phase field (MPF) method [17,18] and the 3D vertex method [19] can be used to calculate the equilibrium particle shape from given anisotropic functions (Wulff plots); the phase-field crystal (PFC) model, which is based on a dynamic density functional theory, can predict the anisotropy of various crystal defects (GBs, TJs, etc.) from given free energy functionals and the correlation functions between different atoms. It enables simulations of heterogeneous nucleation on the atomistic scale [20,21] and, therefore, can facilitate simulations of anisotropic GB nucleation.

3. Energy barrier for nucleation at a grain boundary

The derived equations can be applied to the simplest scenario of nucleation, where the onset of a precipitate at a grain boundary does not involve any intermediate metastable phase and all interfaces are assumed to be incoherent. Those strong presumptions allow us to continue to use the free energy expression of Eq. (3) for the nuclei. Although the reality is usually more complex, it is interesting to compare the nucleation energy in the classical sharp-interface model under different conditions. We already derived the free energy of a particle in equilibrium with a grain boundary (Eq. (12)). Suppose that there are two particles of the same volume and composition, one in the bulk and one at the grain boundary. Their excess free energy, as a function of the nucleus size, is shown in Fig. 5.

With $r = r_v$ the excess free energy of a spherical nucleus embedded in the bulk is given by

$$G(r) = 4\pi \left(\gamma_s r^2 - \frac{1}{3}\Delta p r^3 \right) \tag{16}$$

which yields a "critical radius" r_c,

$$r_c = \frac{2\gamma_s}{\Delta p} \tag{17}$$

The nucleation energy G_{nucl} reads

$$G_{\text{nucl}} = G(r_c) = \frac{4\pi}{3}\gamma_s r_c^2 \tag{18}$$

G_{nucl} changes if nucleation occurs at a grain boundary in particular due to the TJ line tension (Fig. 5). It may require more energy to

form a grain boundary nucleus than in the bulk if the line tension is large enough. In fact, a positive line tension can render heterogeneous nucleation at grain boundaries energetically unfavorable. Zhao et al. [3] suggested that a migrating grain boundary will first try to circumvent a particle rather than intersecting it because of the energy barrier for the formation of the triple line.

For a given critical radius for bulk nucleation $2\gamma_s/\Delta p$, the nucleation energy barrier depends strongly on the TJ tension (Fig. 6). A positive line tension renders GB nucleation energetically unfavorable for particles with a size smaller than $6r^*$. More generally, the critical size for energetically favorable nucleation at a GB is given by $\frac{2\gamma_s}{\gamma_b} \cdot r^*$. For a negative line tension, the curve $G(r_v)$, as shown in (Fig. 5), reaches a local minimum at a point near $r_v = 0$. This negative minimum value G_{min} shows up in Fig. 6 by the curve sections below $G = 0$. This phenomenon is a natural outcome of the assumption that the TJ tension falls below zero. According to Eq. (10), for a negative TJ tension, the particle radius approaches a finite value as the contact angle (particle volume) tends to zero, whence the volume vanishes (Eq. (13)). At this extreme case, the excess free energy of the precipitate is negative according to Eq. (3), in which the second term inside the bracket becomes zero. It is obvious that the effect of the bulk driving force Δp also vanishes if the volume tends to zero. In other words, this kind of precipitate can never be dissolved. To prevent such singularity, the interface thickness and the dependency of TJ tension on the contact angle should be taken into account.

Generally speaking, TJs are one-dimensional defects and grain/phase boundaries are two-dimensional defects. The results of the model can be regarded as the competition between the excess energy of the 1D and 2D defects, where the former is linearly related to the particle radius r and the latter has a quadratic dependency, r^2. With this consideration, similar effects of TJ energy can be expected in more complex systems, such as particles that nucleate along GB junctions of the parent phase. However, in this case the competition between different kinds of TJs should be taken into account.

While the current model is derived from an ideal system with a relatively flat GB (curvature of the particle surface is much larger than the curvature of the GB), it is interesting to consider the situation when the grain/particle size of the parent phase is comparable to or smaller than the critical nucleus size, where the grain/phase boundary fraction is high. Experimental work on the Fe and Au-Fe systems by Amram, Rabkin, et al. [22,23] has shown different phase transformation behavior of nano-/sub-micro particles and films, in comparison to that of the bulk. A "reverse size effect" was observed from the phase transformation in Fe thin films: the phase
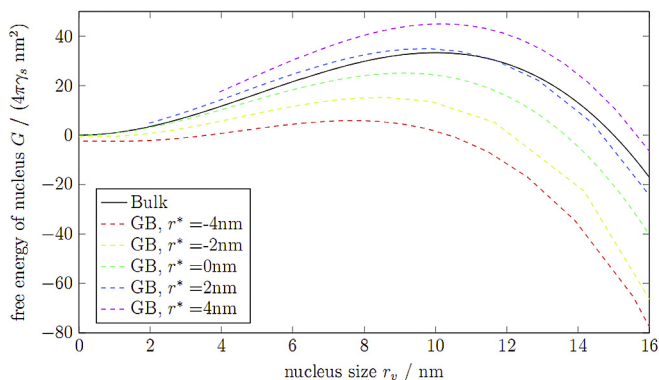

Fig. 5. Dependence of excess free energy of a nucleus in the bulk or at a grain boundary on nucleus size for different line tensions r^*. $\gamma_b/\gamma_s = 1/3$, $2\gamma_s/\Delta p = 10$nm.
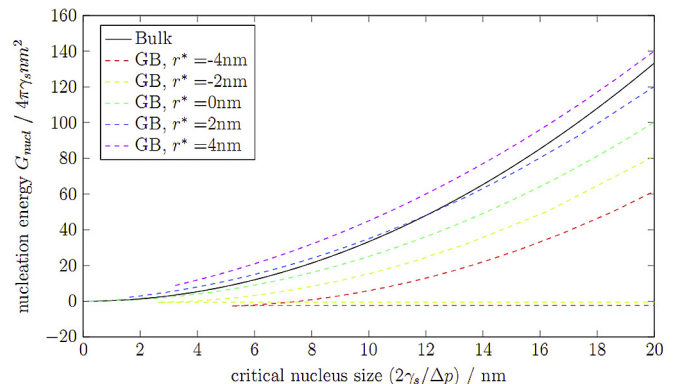

Fig. 6. Comparison of nucleation energy for the nuclei in the bulk or at the grain boundary. $\gamma_b/\gamma_s = 1/3$.

transformation was inhibited in a certain thickness range. They proposed a size-dependent nucleation model such that the nucleation energy barrier is reduced by a smaller particle size. By including the contribution of TJ energy, the size-dependency of the nucleation barrier will be magnified because of the changing contact angle at the three-phase-boundary junctions. The aforementioned size effects arising from a positive TJ line tension imply as well that the nucleation sites can also change with the particle size of the parent phase.

4. Summary

We derived the equilibrium shape of a precipitate at a grain boundary by minimization of the excess energy of the grain boundary, phase boundary, and their triple junction. The excess energy τ of the TJ strongly influences the contact angle and mean curvature of the particle, which results in an additional factor in the exponent of the classical Gibbs-Thomson equation. Numerical studies of this equation demonstrate that the TJ effect becomes dominant for particles with a size smaller or comparable to the "characteristic length" $r^* = \tau/\gamma_s$ (γ_s - interface energy). A positive TJ line tension can increase the energy barrier for GB nucleation compared to that in the bulk when the nucleus size falls below $\frac{2\gamma_s}{\gamma_b} \cdot r^*$. For an appropriate treatment of the nucleation and growth of small particles at the grain boundary, this contribution has to be accounted for and requires a new theoretical approach.

References

[1] J.W. Gibbs, On the equilibrium of heterogeneous substances, Conn. Acad. Arts Sci. 3 (1874–78), 108–248 and 343–524.

[2] B. Zhao, J. Verhasselt, L. Shvindlerman, G. Gottstein, Measurement of grain boundary triple line energy in copper, Acta Mater. 58 (17) (2010) 5646–5653.

[3] B. Zhao, G. Gottstein, L. Shvindlerman, Triple junction effects in solids, Acta Mater. 59 (May 2011) 3510–3518.

[4] S. Eich, G. Schmitz, Embedded-atom study of low-energy equilibrium triple junction structures and energies, Acta Mater. 109 (2016) 364–374.

[5] S. Srinivasan, J. Cahn, H. Jónsson, G. Kalonji, Excess energy of grain-boundary trijunctions: an atomistic simulation study, Acta Mater. 47 (9) (1999) 2821–2829.

[6] M. Upmanyu, D. Srolovitz, L. Shvindlerman, G. Gottstein, Triple junction mobility: a molecular dynamics study, Interface Sci. 7 (3) (1999) 307–319.

[7] M. Upmanyu, D. Srolovitz, L. Shvindlerman, G. Gottstein, Molecular dynamics simulation of triple junction migration, Acta Mater. 50 (6) (2002) 1405–1420.

[8] L.S. Shvindlerman, Laws of Particulate Transition through the Interface (Zakonomernosti Perekhoda Makrochastits Cherez Granitsu Razdela Faz), PhD thesis, 1968. Moscow.

[9] L. Boruvka, A.W. Neumann, Generalization of the classical theory of capillarity, J. Chem. Phys. 66 (12) (1977) 5464–5476.

[10] B.V. Toshev, D. Platikanov, A. Scheludko, Line tension in three-phase equilibrium systems, Langmuir 4 (3) (1988) 489–499.

[11] L.-O. Heim, E. Bonaccurso, Measurement of line tension on droplets in the submicrometer range, Langmuir 29 (46) (2013) 14147–14153.

[12] A. Checco, P. Guenoun, J. Daillant, Nonlinear dependence of the contact angle of nanodroplets on contact line curvature, Phys. Rev. Lett. 91 (Oct 2003) 186101.

[13] A. Caro, H. Van Swygenhoven, Grain boundary and triple junction enthalpies in nanocrystalline metals, Phys. Rev. B 63 (Feb 2001) 134101.

[14] Y. Liu, J. Wang, X. Zhang, Accurate determination of the vapor-liquid-solid contact line tension and the viability of young equation, Sci. Rep. 3 (Jun 2013).

[15] C.A. Ward, J. Wu, Effect of contact line curvature on solid-fluid surface tensions without line tension, Phys. Rev. Lett. 100 (Jun 2008) 256103.

[16] C. Delaunay, Sur la surface de revolution dont la courbure moyenne est constante, J. Math. Pures Appl. 6 (1841) 309–320.

[17] I. Steinbach, O. Shchyglo, Phase-field modelling of microstructure evolution in solids: perspectives and challenges, Curr. Opin. Solid State Mater. Sci. 15 (3) (2011) 87–92, http://dx.doi.org/10.1016/j.cossms.2011.01.001.

[18] W. Guo, R. Spatschek, I. Steinbach, An analytical study of the static state of multi-junctions in amulti-phase field model, Phys. D Nonlinear Phenom. 240 (4–5) (2011) 382–388, http://dx.doi.org/10.1016/j.physd.2010.09.014.

[19] C. Miessen, M. Liesenjohann, L.A. Barrales-Mora, L.S. Shvindlerman, G. Gottstein, An advanced level set approach to grain growth - accounting for grain boundary anisotropy and finite triple junction mobility, Acta Mater. 99 (2015) 39–48, http://dx.doi.org/10.1016/j.actamat.2015.07.040.

[20] L. Granasy, F. Podmaniczky, G.I. Toth, G. Tegze, T. Pusztai, Heterogeneous nucleation of/on nano particles: a density functional study using the phase-field crystal model, Chem. Soc. Rev. 43 (7) (2014) 2159–2173, http://dx.doi.org/10.1039/C3CS60225G.

[21] M. Greenwood, N. Ofori-Opoku, J. Rottler, N. Provatas, Modeling structural transformations in binary alloys with phase field crystals, Phys. Rev. B 84 (2011) 064104, http://dx.doi.org/10.1103/PhysRevB.84.064104.

[22] D. Amram, E. Rabkin, Phase transformations in Au-Fe particles and thin films: size effects at themicro- and nano-scales, JOM 68 (5) (2016) 1335–1342, http://dx.doi.org/10.1007/s11837-016-1847-8.

[23] D. Amram, O. Kovalenko, E. Rabkin, The alpha-gamma transformation in Fe and Fe-Au thin films, micro- and nanoparticles — an in situ study, Acta Mater. 98 (2015) 343–354, http://dx.doi.org/10.1016/j.actamat.2015.07.051.